Multivariate Analysis by the Minimum Spanning Tree Method of the Structural Determinants of Diphenylethylenes and Triphenylacrylonitriles Implicated in Estrogen Receptor Binding, Protein Kinase C Activity, and MCF_7 Cell Proliferation†

Jean-Christophe Doré,*,‡ Jacques Gilbert,§ Eric Bignon,∥,# André Crastes de Paulet,∥ Tiiu Ojasoo,⊥ Michel Pons,∥ Jean-Pierre Raynaud,⊥,# and Jean-François Miquel§,#

CNRS URA 401, Muséum National d'Histoire Naturelle, 75005 Paris, France, CNRS-CERCOA, 94320 Thiais, France, INSERM U58, 34100 Montpellier, France, and Roussel-UCLAF, 75007 Paris, France. *Received September 30, 1991*

The response profiles of 36 para-substituted diphenylethylenes (DPEs) and triphenylacrylonitriles (TPEs) have been compared by multivariate analysis. The responses measured were (a) relative binding affinity (RBA) for the cytosol estrogen receptor (ER), (b) ability to promote the growth of the human MCF_7 breast cancer cell-line, (c) cytotoxicity in MCF_7 cells, and (d) ability to stimulate or inhibit protein kinase C (PKC) III activity under three different conditions of enzyme activation. The prime object of the analysis was to observe the simultaneous influence of diverse combinations of substituents on all these in vitro responses. To do this, the minimum spanning tree (MST) method was used to organize the molecules into a network in which proximate molecules are closely related with regard to their responses whereas remote molecules are distinct. The MST of this population of molecules had four main branches. E_2 and its TPE mime were located in a central position within the trunk whereas the tips of the branches tended toward molecules of different specificity, i.e., cytotoxic molecules that bind to ER and interfere with PKC, noncytotoxic molecules that also bind to ER and interfere with PKC but promote cell growth, molecules only active on PKC, and molecules active on all parameters except PKC stimulation. A parallel MST analysis of the relationships among the response parameters themselves confirmed previous conclusions: For this population of molecules, RBAs for ER are fairly closely related to ability to promote MCF_7 cell growth and only little to cytotoxicity (Bignon et al. *J. Med. Chem.* **1989**, *32*, 2092). Cytotoxicity is much more clearly correlated with inhibition of diacylglycerol-stimulated PKC activity than with RBAs for ER. PKC inhibition differs substantially depending upon whether the substrate is H_1 histone or protamine sulfate.

Introduction

Present day antihormonal treatment of metastatic breast cancer relies heavily on the use of a single nonsteroid antiestrogen, tamoxifen, that belongs to the class of the triphenylethylene (TPE) derivatives.[1-3] Tamoxifen, its metabolites, and analogues have been reported to have many molecular targets including a nuclear receptor (the estrogen receptor (ER)),[4] membrane receptors (possibly the histamine,[5] dopamine, and muscarinic receptors), a primarily microsomal antiestrogen binding protein,[6-8] several enzymes (prostaglandin synthase,[9] glutamate deshydrogenase[10]) including at least two Ca^{2+}-dependent kinases (calmodulin kinase[11] and protein kinase C (PKC)[12-19]). The relevance of interaction with these targets to growth-promotion or inhibition is not yet fully understood.

Several structural analogues of tamoxifen have been designed,[2,3] at least two of which (i.e. toremifene,[20] droloxifene[21]) are in clinical development. These compounds with slightly different activity profiles can inhibit the growth of certain tamoxifen-resistant tumors. New steroidal antiestrogens with bulky or lengthy substituents in either C-11,[22-26] C-7,[27-29] or C-17[30-32] are also under investigation.

Because the majority, if not all, patients with malignant endocrine tumors (e.g. breast and prostate cancer) will become resistant to hormone therapy and relapse, a choice of potent antitumor agents that interfere with multiple molecular targets implicated in cell proliferation is desirable. This, however, implies an ability to compare not just

† This work was presented at the 73rd Annual Meeting of the Endocrine Society (Washington, June 19-22, 1991). Abstract No. 571, p 173.

‡ CNRS URA 401.

§ CNRS-CERCOA.

∥ INSERM U58.

⊥ Roussel-UCLAF.

Present address: E.B., SANOFI, 31036 Toulouse Cedex, France; J.-F.M., LEPI, 75020 Paris, France; J.-P.R., 51 bd Suchet, 75016 Paris, France.

(1) Buckley, M. M.; Goa, K. L. Tamoxifen. A reappraisal of its pharmacodynamic and pharmacokinetic properties, and therapeutic use. *Drugs* **1989**, *37*, 451.

(2) Jordan, V. C.; Murphy, C. S. Endocrine pharmacology of antiestrogens as antitumor agents. *Endocr. Rev.* **1990**, *11*, 578.

(3) Miquel, J. F.; Gilbert, J. A chemical classification of nonsteroidal antagonists of sex-steroid hormone action. *J. Steroid Biochem.* **1988**, *31*, 525.

(4) Coezy, E.; Borgna, J. L.; Rochefort, H. Tamoxifen and metabolites in MCF7 cells: correlation between binding to estrogen receptor and inhibition of cell growth. *Cancer Res.* **1982**, *42*, 317.

(5) Brandes, L. J.; Bogdanovic, R. P. New evidence that the antiestrogen binding site may be a novel growth-promoting histamine receptor which mediates the antiestrogenic and antiproliferative effects of tamoxifen. *Biochem. Biophys. Res. Commun.* **1986**, *134*, 601.

(6) Lazier, C. B.; Bapat, B. V. Antiestrogen binding sites: general and comparative properties. *J. Steroid Biochem.* **1988**, *31*, 665.

(7) Tang, B. L.; Teo, C. C.; Sim, K. Y.; Ng, M. L.; Kon, O. L. Cytostatic effect of antiestrogens in lymphoid cells: relationship to high affinity antiestrogen-binding sites and cholesterol. *Biochim. Biophys. Acta* **1989**, *1014*, 162.

(8) Poirot, M.; Garnier, M.; Bayard, F.; Rivière, I.; Traore, M.; Wilson, M.; Fargin, A.; Faye, J. C. The anti-proliferative properties of 4-benzylphenoxy ethanamine derivatives are mediated by the anti-estrogen binding site (ABS), whereas the antiestrogenic effects of trifluopromazine are not. *Biochem. Pharmacol.* **1990**, *40*, 425.

(9) Gilbert, J.; Miquel, J. F.; Précigoux, G.; Hospital, M.; Raynaud, J. P.; Michel, F.; Crastes de Paulet, A. Inhibition of prostaglandin synthetase by di- and triphenylethylene derivatives: A structure-activity study. *J. Med. Chem.* **1983**, *26*, 693.

(10) Pons, M.; Michel, F.; Descomps, B.; Crastes de Paulet, A. Structural requirements for maximal inhibitory allosteric effect of estrogens and estrogen analogues on glutamate dehydrogenase. *Eur. J. Biochem.* **1978**, *84*, 257.

0022-2623/92/1835-0573$03.00/0 © 1992 American Chemical Society

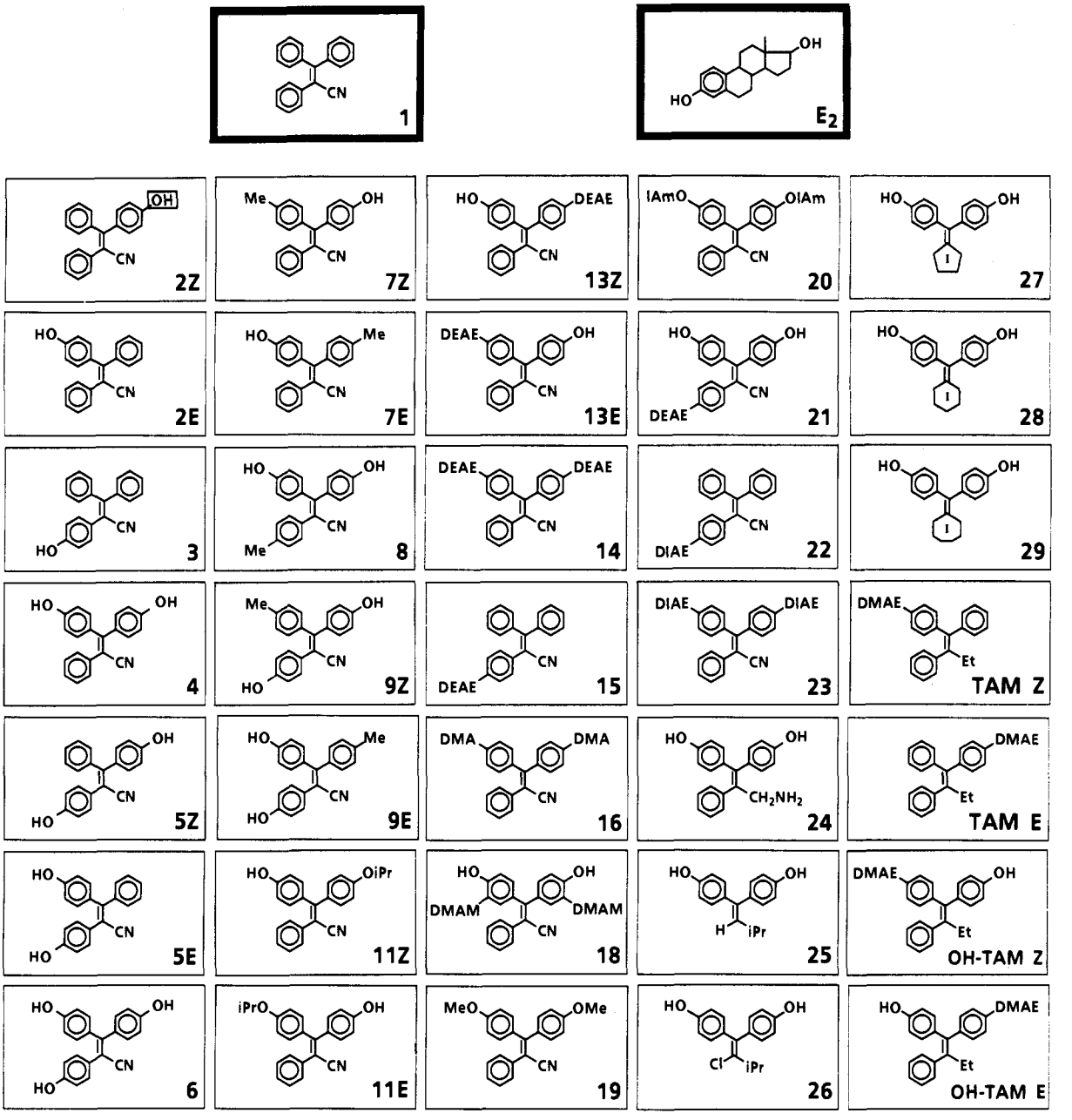

Figure 1. Structures and code numbers of the test molecules.

a single activity but the overall response profiles of series of test compounds, i.e. interaction with these molecular targets, inhibition of hormone-dependent and -independent cell-lines, cytotoxicity, etc.

(11) Barrera, G.; Screpanti, I.; Paradisi, L.; Parola, M.; Ferretti, C.; Vacca, A.; Farina, A.; Dianzani, M. U.; Frati, L.; Gulino, A. Structure-activity relationships of calmodulin antagonism by triphenylethylene antiestrogens. *Biochem. Pharmacol.* **1986**, *35*, 2984.

(12) O'Brian, C. A.; Liskamp, R. M.; Solomon, D. H.; Weinstein, I. B. Inhibition of protein kinase C by tamoxifen. *Cancer Res.* **1985**, *45*, 2462.

(13) O'Brian, C. A.; Liskamp, R. M.; Solomon, D. H.; Weinstein, I. B. Triphenylethylenes: a new class of protein kinase C inhibitors. *J. Natl. Cancer Inst.* **1986**, *76*, 1243.

(14) Su, H. D.; Mazzei, G. J., Vogler, W. R.; Kuo, J. F. Effect of tamoxifen, a nonsteroidal antiestrogen, on phospholipid/calcium- dependent protein kinase and phosphorylation of its endogenous substrate proteins from the rat brain and ovary. *Biochem. Pharmacol.* **1985**, *34*, 3649.

(15) Horgan, K.; Cooke, E.; Hallett, M. B.; Mansel, R. E. Inhibition of protein kinase C mediated signal transduction by tamoxifen. Importance for antitumor activity. *Biochem. Pharmacol.* **1986**, *35*, 4463.

(16) Bignon, E.; Ogita, K.; Kishimoto, A.; Gilbert, J.; Abecassis, J.; Miquel, J. F.; Nishizuka, Y. Modes of inhibition of protein kinase C by triphenylacrylonitrile anti-estrogens. *Biochem. Biophys. Res. Commun.* **1989**, *163*, 1377.

(17) Bignon, E.; Kishimoto, A.; Pons, M.; Crastes de Paulet, A.; Gilbert, J.; Miquel, J. F.; Nishizuka, Y. Dual action of hydroxylated diphenylethylene estrogens on protein kinase C. *Biochem. Biophys. Res. Commun.* **1990**, *166*, 1471.

(18) Bignon, E.; Pons, M.; Gilbert, J.; Nishizuka, Y. Multiple mechanisms of protein kinase C inhibition by triphenylacrylonitrile antiestrogens. *Febs Lett.* **1990**, *271*, 54.

(19) Bignon, E.; Ogita, K.; Kishimoto, A.; Nishizuka, Y. Protein kinase C subspecies in estrogen receptor-positive and -negative human breast cancer cell lines. *Biochem. Biophys. Res. Commun.* **1990**, *171*, 1071.

(20) Kangas, L.; Baum, M. (Eds) Proceedings of the Toremifene Symposium. UICC World Cancer Congress, Budapest. *J. Steroid Biochem.* **1990**, *36*, 191.

(21) Pritchard, K. (Ed) Droloxifene, a new antiestrogen with therapeutic advantages. Symposium Proceedings, International Cancer Congress. *Am. J. Clin. Oncol.*, in press.

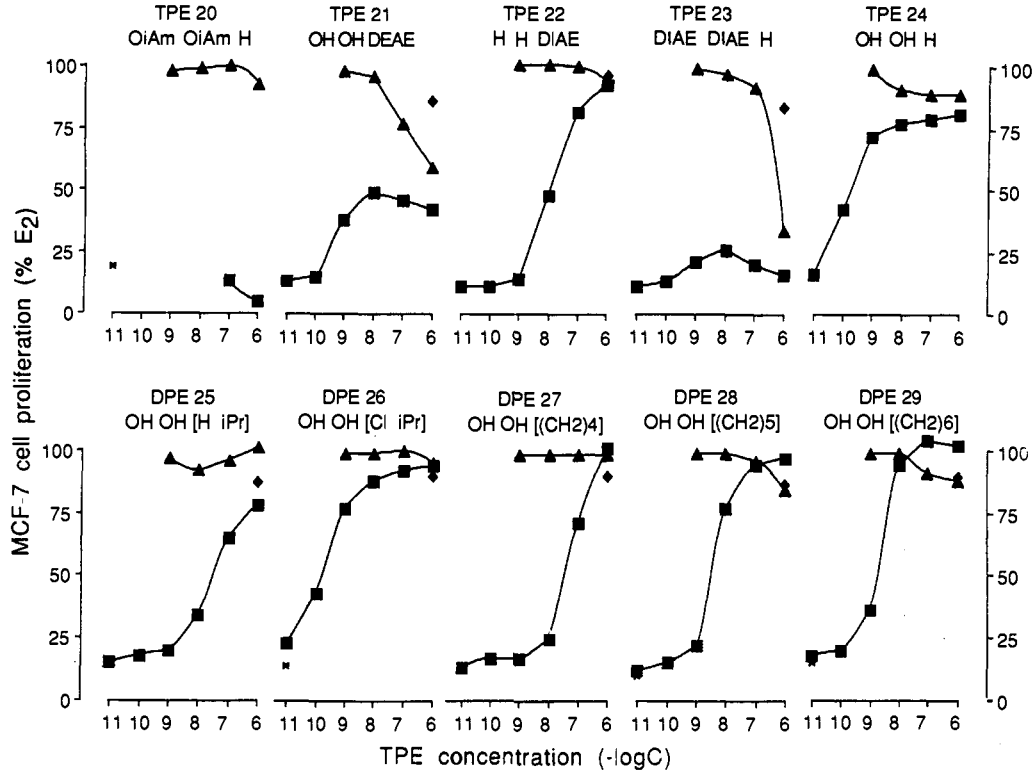

Figure 2. Stimulation and inhibition by TPEs and DPEs of MCF_7 cell proliferation in the absence (■) or presence (▲) of 0.1 nM estradiol. Rescue of cells by 100 nM E_2 is indicated by the sign ♦. Results (mean of triplicate wells from a typical experiment, SD < 5%) are expressed as percent DNA after 8 days of growth in the presence of 0.1 nM estradiol (Percent DNA = 100 × (μg of DNA TPE/μg of DNA E_2). Test compounds are identified by their number and their α,α′,β-substituents. (The substitutions on the double bond of DPEs are indicated in brackets.) An asterisk (*) indicates a control value (vehicle alone).

In previous papers, we have investigated the action of a large number of triphenylacrylonitriles on several biochemical and biological parameters[33-35] and, in particular, on relative binding affinity (RBA) for ER, ability to promote human breast cancer (MCF_7) cell growth and to inhibit estradiol (E_2)-promoted cell growth, cytotoxicity in these ER-positive cells and in ER-negative (BT_{20}) cells,[36] and stimulation or inhibition of PKC activity.[37] The data have been submitted to a multivariate factorial analysis (correspondence analysis) in order to discern possible relationships among the biological variables.[38] In this paper,

(22) Raynaud, J. P.; Ojasoo, T.; Bouton, M. M.; Bignon, E.; Pons, M.; Crastes de Paulet, A. Structure-activity relationships of steroid estrogens. In *Estrogens in the Environment*; McLachlan, J. A., Ed.; Elsevier: Amsterdam, 1985; p 24.
(23) Raynaud, J. P.; Ojasoo, T. The design and use of sex-steroid antagonists. *J. Steroid Biochem.* **1986**, *25*, 811.
(24) Jordan, V. C.; Koch, R. Regulation of prolactin synthesis in vitro by estrogenic and antiestrogenic derivatives of estradiol and estrone. *Endocrinology* **1989**, *124*, 1717.
(25) Robinson, S. P.; Jordan, V. C. The paracrine stimulation of MCF-7 cells by MDA-MB-231 cells: possible role in antiestrogen failure. *Eur. J. Cancer Clin. Oncol.* **1989**, *25*, 493.
(26) Claussner, A.; Nédélec, L.; Nique, F.; Philibert, D.; Teutsch, G.; Van de Velde, P. 11β-amidoalkyl estradiols, a new series of pure antiestrogens. *J. Steroid Biochem. Mol. Biol.*, in press.
(27) Wakeling, A. E.; Bowler, J. Novel antioestrogens without partial agonist activity. *J. Steroid Biochem.* **1988**, *31*, 645.
(28) Weatherill, P. J.; Wilson, A. P. M.; Nicholson, R. I.; Davies, P.; Wakeling, A. E. Interaction of the antioestrogen ICI 164,384 with the estrogen receptor. *J. Steroid Biochem.* **1988**, *30*, 263.
(29) Wakeling, A. E. Comparative studies on the effects of steroidal and nonsteroidal oestrogen antagonists on the proliferation of human breast cancer cells. *J. Steroid Biochem.* **1989**, *34*, 183.
(30) Poulin, R.; Mérand, Y.; Poirier, D.; Levesque, C.; Dufour, J. M.; Labrie, F. Antiestrogenic properties of keoxifene, trans-4-hydroxytamoxifen, and ICI 164384, a new steroidal antiestrogen, in ZR-75-1 human breast cancer cells. *Breast Cancer Res. Treat.* **1989**, *14*, 65.
(31) Poirier, D.; Labrie, C.; Mérand, Y.; Labrie, F. Derivatives of ethynylestradiol with oxygenated 17α-alkyl side chain: synthesis and biological activity. *J. Steroid Biochem.* **1990**, *36*, 133.
(32) Poirier, D.; Labrie, C.; Mérand, Y.; Labrie, F. Synthesis and biological activity of 17α-alkynylamide derivatives of estradiol. *J. Steroid Biochem. Molec. Biol.* **1991**, *38*, 759.
(33) Pons, M.; Michel, F.; Crastes de Paulet, A.; Gilbert, J.; Miquel, J. F.; Précigoux, G.; Hospital, M.; Ojasoo, T.; Raynaud, J. P. Influence of new hydroxylated triphenylethylene (TPE) derivatives on estradiol binding to uterine cytosol. *J. Steroid Biochem.* **1984**, *20*, 137.
(34) Pons, M.; Michel, F.; Bignon, E.; Crastes de Paulet, A.; Gilbert, J.; Miquel, J. F.; Précigoux, G.; Hospital, M.; Ojasoo, T.; Raynaud, J. P. A rational approach to the design of antiestrogens: The case of hydroxylated triphenylethylene derivatives. In *Hormones and Cancer 2, Progress Cancer Research Therapy* 31; Bresciani, F., et al., Eds.; Raven Press: New York, 1984; p 27.
(35) Bignon, E.; Pons, M.; Gilbert, J.; Crastes de Paulet, A. Analogies and differences in the modulation of progesterone receptor induction and cell proliferation by estrogens and antiestrogens in MCF-7 breast cancer cells: study with 24 triphenylacrylonitrile derivatives. *J. Steroid Biochem.* **1988**, *31*, 877.
(36) Bignon, E.; Pons, M.; Crastes de Paulet, A.; Doré, J. C.; Gilbert, J.; Abecassis, J.; Miquel, J. F.; Ojasoo, T.; Raynaud, J. P. Effect of triphenylacrylonitrile derivatives on estradiol-receptor binding and on human breast cancer cell growth. *J. Med. Chem.* **1989**, *32*, 2092.
(37) Bignon, E.; Pons, M.; Doré, J. C.; Gilbert, J.; Ojasoo, T.; Miquel, J. F.; Raynaud, J. P.; Crastes de Paulet, A. Influence of di- and tri-phenylethylene estrogen/antiestrogen structure on the mechanisms of protein kinase C inhibition and activation as revealed by a multivariate analysis. *Biochem. Pharmacol.* **1991**, *42*, 1373.

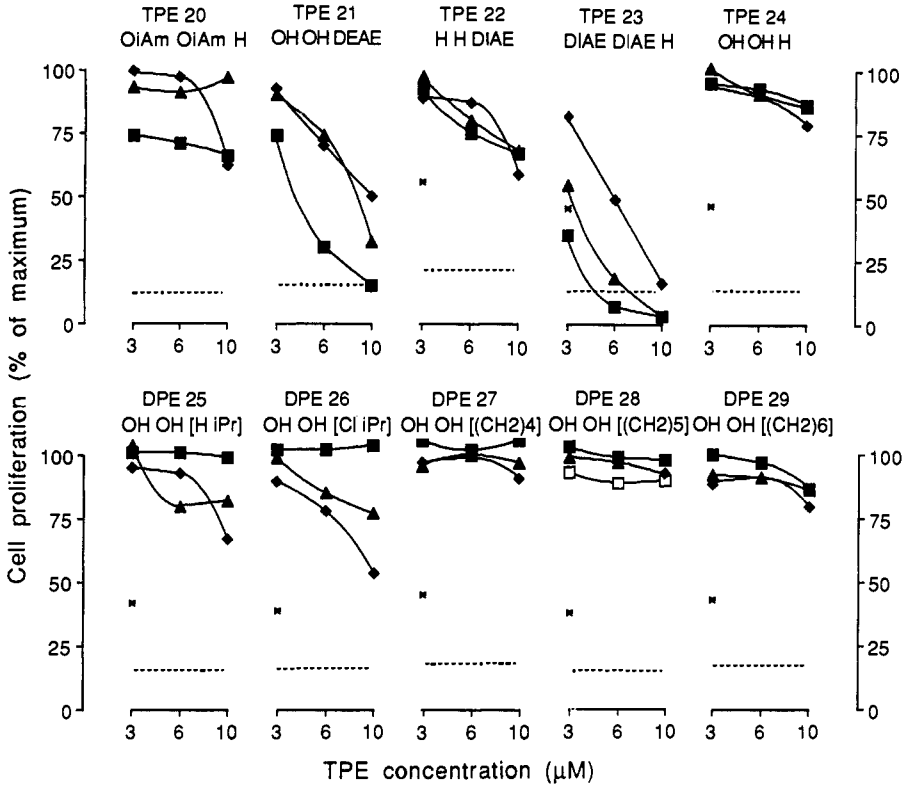

Figure 3. Effect of high TPE or DPE concentrations (3–10 μM) on the proliferation of MCF_7 and BT_{20} cells. Results for triplicate wells from a typical experiment are expressed as percent DNA after 6 days growth in the presence of 1 μM E_2 for the MCF_7 cells (=[(μg of DNA TPE)/(μg of DNA E_2)] × 100) and as a function of the control for the BT_{20} cells (=[(μg of DNA TPE)/(μg of DNA control)] × 100): (■) MCF_7 + TPE, (▲) MCF_7 + 1 μM E_2 + TPE, (*) MCF_7 control, (♦) BT_{20} + TPE, (- - -) level of seeding for MCF_7 cells. The seeding level was 20–30% for BT_{20} cells; 100% corresponded to about 7–10 and 3 μg of DNA for MCF_7 and BT_{20} cells, respectively.

our aim is to analyze the combinations of structural features that might be directly implicated in some of these activities by another multivariate method (i.e. by cluster analysis by the minimum spanning tree (MST)).[39]

Results and Discussion

Chemistry. The synthesis of all compounds (Figure 1) except **20–23** has been described.[33,36,40,41] Compound **20** was obtained by reaction of 1-bromo-3-methylbutane with the disodium derivative of 2-phenyl-3,3-bis(4-hydroxyphenyl)acrylonitrile; compound **21** by condensation of [4-[2-(diethylamino)ethoxy]phenyl]acetonitrile with 4,4′-bis(tetrahydropyran-2-yloxy)benzophenone in the presence of sodium amidure with subsequent release of the two OH groups; compounds **22** and **23** by condensation of (diisopropylamino)ethyl chloride respectively with the sodium derivative of 2-(4-hydroxyphenyl)-3,3-diphenylacrylonitrile and the disodium derivative of 2-phenyl-3,3-bis(4-hydroxyphenyl)acrylonitrile.

Estrogen Receptor (ER) Binding of New Compounds: Action on Cell Proliferation. The biological activity profiles of all compounds except **20–29** have been published with regard to ER binding and cell proliferation.[36] The activities of **20–29** are described below (Table I).

Apart from compounds **20**, **22**, and **23** which lack α,α′-hydroxy groups, all the other test compounds competed noticeably for labeled E_2 binding. The most powerful competitors in Table I were isopropyl-substituted DPEs (**25**, **26**), but their RBAs did not attain the values previously recorded for certain α,α′-dihydroxylated TPEs (e.g TPEs **4**, **6**, **8** in Table II). The presence of a DEAE on ring β of a α,α′-dihydroxylated TPE (**21** vs **4**) decreased the RBA 24-fold. On the other hand, in the DPE series, a chlorine atom linked to the double bond in lieu of a hydrogen reinforced the stability of binding (**25** vs **26**).

In our assay medium which contained no phenol red, E_2 promoted the growth of MCF_7 cells 5–10-fold over control, giving a dose–response curve with a maximum at 0.1 nM. In the absence of E_2 the cells hardly grew (doubling time = 110–120 h). All the new test compounds except **20**, which has no affinity for ER, could stimulate proliferation over the concentration range 10 pM to 1 μM (Figure 2). Several (**22**, **26–29**) induced a maximum response approaching that of E_2 (agonist effect of 93–100%), but with widely different EC_{50}s (0.16–130 nM). Others (**21** and **24**) displayed only partial agonist activity as already observed[36] with α,α′-dihydroxylated TPEs (**4**, **6**, **8**) (see Table II).

Only **21** and **23** could substantially decrease the proliferation induced by 0.1 nM E_2 in a concentration-dependent manner (triangles in Figure 2), the more inhibitory of the two being **23** with basic amino side chains in α,α′-positions. Both these compounds also had some agonist activity. The mixed agonist/antagonist properties of **21** which are comparable to those of **4**[36] can be explained by its α,α′-dihydroxylated structure. Inhibition of prolifera-

(38) Ojasoo, T.; Bignon, E.; Crastes de Paulet, A.; Dorê, J. C.; Gilbert, J.; Miquel, J. F.; Pons, M.; Raynaud, J. P. Relative involvement of the estrogen receptor and protein kinase C in the action of a population of triphenylethylenes on MCF_1 cell proliferation as revealed by correspondence factorial analysis (CFA). *Mol. Pharmacol.*, submitted for publication.

(39) Prim, R. C. Shortest connection networks and some generalisations. *Bell Syst. Technol. J.* **1957**, *36*, 1389.

(40) Miquel, J. F.; Wahlstam, H.; Olsson, K.; Sunbeck, J. Synthesis of unsymmetrical diphenylalkenes. *J. Med. Chem.* **1963**, *6*, 774.

(41) Miquel, J. F.; Sékéra, A.; Chaudron, T. Synthèse de polyphénylèthylènes et interférences avec le récepteur oestrogène d'utérus de souris (Synthesis of polyphenylethylenes and their action on mouse uterus estrogen receptor). *C. R. Acad. Sci. Serie C (Paris)* **1978**, *286*, 151.

Table I. Physical, Biochemical, and Biological Properties of 3,3,2-Triphenylacrylonitriles and Diphenylethylenes

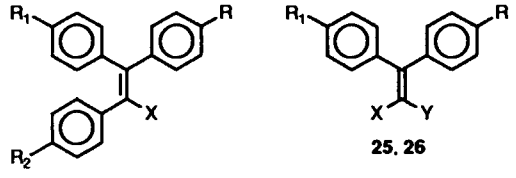

20–24

25, 26

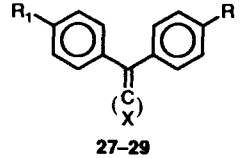

27–29

TPE/ DPE	structure X	Y	R(α)	$R_1(\alpha')$	$R_2(\beta)$	mp, °C	formula	anal. or ref	ER binding RBA (%) (2 h at 0 °C)	ER binding RBA (%) (5 h at 25 °C)	MCF_7 cell proliferation agonism EC_{50} (nM)	%	antagonism IC_{50} (nM)	%	cyto IC_{30} (μM)	%	cyto BT_{20} IC_{30} (μM)	%
20	CN		OiAM	OiAm	H	111	$C_{31}H_{35}NO_2$	C,H,N	nd[a]	<0.01	>1000	0	>1000	0	>10	3	9	37
21	CN		OH	OH	DEAE	135–7	$C_{27}H_{28}N_2O_3$	C,H,N	nd	2.5	0.5–0.8	45	200	50	6	68	3	50
22	CN		H	H	DIAE	*c*	$C_{29}H_{32}N_2O$	C,H,N	0.1	0.01	11	93	nm[b]	10	10	30	9	36
23	CN		DIAE	DIAE	H	*d*	$C_{37}H_{49}N_3O_2$	C,H,N	0.03	0.03	0.84	29	325	79	2.7	97	3.2	89
24	CH_2NH_2		OH	OH	H	110–2	$C_{21}H_{19}NO_2$	[41]	9.7	12	0.14	76	nm	20	nm	19	20	24
25	H	iPr	OH	OH		174	$C_{17}H_{18}O_2$	[41]	58	4.2	18	65	nm	5	nm	22	8.4	40
26	Cl	iPr	OH	OH		176–8	$C_{17}H_{17}ClO_2$	[41]	70	36	0.16	96	nm	12	nm	30	7.6	45
27	$(CH_2)_4$		OH	OH		197	$C_{18}H_{18}O_2$	[41]	23	0.84	130	100	nm	1	nm	6	nm	10
28	$(CH_2)_5$		OH	OH		235	$C_{18}H_{20}O_2$	[41]	26	2.6	4.51	97	nm	23	nm	12	nm	12
29	$(CH_2)_6$		OH	OH		195–8	$C_{20}H_{22}O_2$	[40]	17	2.9	2.65	96	nm	21	nm	16	nm	20

[a] Nd: not determined. [b] Nm: not measurable. [c] Bp $E_{0.01}$ 250–5 °C. [d] Isolated and purified as an oil by chromatography on silica gel. The relative binding affinities (RBAs), determined under two sets of incubation conditions, are the means of at least four experimental values. The effective (EC_{50}) and inhibitory (IC_{50}) concentrations giving 50% of the maximum response of the TPE were determined in two separate experiments. The percent agonist effect is expressed as a function of the maximum response recorded with E_2; the percent antagonist effect is the percent inhibition obtained at 10^{-6} M TPE versus 10^{-10} M E_2. The IC_{30} is the concentration that inhibits cell proliferation (cyto) by 30% in the absence (BT_{20}) or presence of 10^{-6} M E_2 (MCF_7). The percent inhibition is that obtained in the presence of 10^{-5} M TPE. The results are the means of two experiments.

Table II. Biological Effects of TPEs and DPEs (Percent of Control): Calf Uterus ER Binding, MCF_7 Cell Proliferation, and Rat Brain PKC III Activity

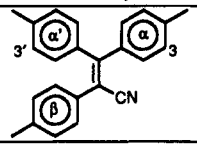

	structure			ER binding RBA	MCF_7 cell proliferation		PKC III activity		
	α	α'	β	(5 h at 25 °C)	agonism	cyto	PS	PS+DO	prot. s.
1	H	H	H	0.09	68	16	126	106	106
2*Z*	OH	H	H	36	94	12	96	104	94
2*E*	H	OH	H	2.2	99	30	107	87	90
3	H	H	OH	3.3	90	8	92	113	103
4	OH	OH	H	62	62	30	94	42	50
5*Z*	OH	H	OH	74	98	17	94	87	86
5*E*	H	OH	OH	6.1	100	30	97	91	68
6	OH	OH	OH	166	85	39	38	32	33
7*Z*	OH	CH_3	H	28	55	38	107	95	77
7*E*	CH_3	OH	H	2.5	53	60	119	87	111
8	OH	OH	CH_3	93	71	38	84	38	46
9*Z*	OH	CH_3	OH	78	69	35	113	80	90
9*E*	CH_3	OH	OH	9.1	73	54	88	68	94
10*Z*	OCH_3	OH	H	0.66	26	36	100	100	100
10*E*	OH	OCH_3	H	17	25	13	100	100	100
11*Z*	OiPr[a]	OH	H	0.36	33	61	138	101	86
11*E*	OH	OiPr	H	6.4	22	57	170	94	79
12	OiPr	OiPr	H	0.01	40	32	100	100	100
13*Z*	DEAE[b]	OH	H	3.4	12	89	10	1	88
13*E*	OH	DEAE	H	108	16	77	20	2	85
14	DEAE	DEAE	H	0.40	62	94	20	10	101
15	H	H	DEAE	0.17	71	53	43	20	96
16	DMA[c]	DMA	H	0.12	85	48	67	57	88
18	OH	OH	H	0.30	31	36	26	23	96
	3DMAM[d]	3DMAM							
19	OCH_3	OCH_3	H	0.17	34	8	98	100	92
20	OiAm[e]	OiAm	H	<0.01	0	3	118	86	78
21	OH	OH	DEAE	2.5	45	68	7	0	105
22	H	H	DIAE	0.01	93	30	46	23	103
23	DIAE[f]	DIAE	H	0.03	29	97	18	8	85
24				12	76	19	78	53	20
25				4.2	65	22	187	70	95
26	see Table I for 24–29			36	96	30	226	83	85
27				0.84	100	6	155	42	40
28				2.6	97	12	111	81	91
29				2.9	96	16	195	71	93
TAM *Z*[g]	H	DMAE	H	1.1	21	49	49	21	107
TAM *E*[g]	DMAE[h]	H	H	0.02	100	79	36	30	93
4-OH-TAM *Z*[g]	OH	DMAE	H	243	10	81	27	2	94
4-OH-TAM *E*[g]	DMAE	OH	H	2.28	61	74	32	14	100
E_2				100	100	25	77	89	99

[a] OiPr: $OCH(CH_3)_2$. [b] DEAE: $O(CH_2)_2N(C_2H_5)_2$. [c] DMA: $N(CH_3)_2$. [d] DMAM: $CH_2N(CH_3)_2$. [e] OiAm: $O(CH_2)_2CH(CH_3)_2$. [f] DIAE: $O(CH_2)_2N(CH(CH_3)_2)_2$. [g] TAM: tamoxifen (C_2H_5 instead of CN). [h] DMAE: $O(CH_2)_2N(CH_3)_2$. The relative binding affinities (RBAs) for ER are the means of at least four experimental values (RBA for E_2 = 100). The percent agonist effect on MCF_7 cell proliferation is a function of the maximum response recorded with E_2 (=100%) whatever the TPE concentration. The percent inhibition of MCF_7 cell proliferation (cyto) is that obtained with 10^{-5} M TPE in the presence of 10^{-9} M E_2. The percent stimulation or inhibition of PKC III activity was determined in the presence of 10^{-4} M of most of the TPEs or DPEs either using H_1 histone as a substrate in the presence of Ca^{2+} and 2 μg/mL phosphatidylserine (PS) with or without 0.2 μg/mL diolein (DO), or using protamine sulfate (prot. s.) as a substrate in the presence of 0.5 mM EGTA instead of Ca^{2+}, PS, and DO.

tion by **21** and **23** could be reversed by addition of 100 nM E_2 (diamonds in Figure 2). A bulky basic amino side chain on the β ring as in **21** did not necessarily generate antagonist properties since TPEs **22** and **15** (see Table II) were agonists only.

The inhibitory action of high TPE concentrations (up to 10 μM) on MCF_7 cell proliferation, reminiscent of a cytostatic and/or cytolytic effect, was first measured under conditions that were unlikely to implicate ER, since the E_2 concentration (10^{-9} M) added could offset the antiestrogenic activity of the TPEs present at a 10-fold higher concentration (10^{-5} M) (Figure 3). The most potent compounds were yet again **21** and **23** followed by **22** whose bulky (diethylamino)ethoxy side chain is no doubt instrumental in generating this inhibition. In the absence of E_2, the cytostatic action of the test compounds blunted any ER-mediated growth stimulation (squares in Figure 3). Analogous antiproliferative effects were recorded in ER-negative BT_{20} cells (diamonds in Figure 3). As already shown for previously studied TPEs,[36] the inhibition curves between 3 and 10 μM in BT_{20} cells were often parallel to those obtained in MCF_7 cells in the presence of 10 μM E_2 (triangles in Figure 3).

Biological Screening Data: ER Binding, Cell Proliferation, PKC Inhibition, or Stimulation. Comparative data are available for 37 test compounds and 7 biological variables relating to ER binding, cell proliferation, cytotoxicity, and PKC III (α) activity.[36,37] PKC, a Ca^{2+}- and phospholipid-dependent enzyme activated by diacylglycerol, is a protein kinase involved in cell surface transduction and in the control of cell proliferation and tumor promotion.[42-44] It phosphorylates many substrates

(42) Inoue, M.; Kishimoto, A.; Takai, Y.; Nishizuka, Y. Studies on a cyclic nucleotide-independent protein kinase and its proenzyme in mammalian tissues. II: Proenzyme and its activation by calcium-dependent protease from rat brain. *J. Biol. Chem.* 1977, *252*, 7610.

including RNA polymerase II, the EGF receptor, and several oncogene proteins which have been directly or inversely related to estrogen action. PKC III activity was measured under different experimental conditions. On the one hand, using histone as a substrate in the presence of phosphatidylserine (PS) and Ca^{2+} in which case maximal enzyme activity is obtained in the presence of the physiological activator, diacylglycerol, on the other hand, using protamine sulfate as a substrate in which case the enzyme activity is Ca^{2+} and phospholipid independent. The results for six of the seven biological variables are given in Table II. The seventh variable arises from splitting the PS column into inhibition and stimulation of PKC activity, since it was noted that several DPEs and TPEs could noticeably stimulate enzyme activity.

Multivariate Analysis by the Minimum Spanning Tree Method. Methodological Principles. Most comparisons of molecules such as the above rely on their *prior* definition in one of the following terms: (i) 3D structures (Dreiding models; van der Waals spheres that, like any other solid, can be translated into contours, vectors, pixel densities, skeletons, etc.; crystalline coordinates), (ii) chemical formulae, to be compared integrally by fitting or as fragments by, for instance, autocorrelation descriptors[45] or DARC-PELCO,[46] (iii) spectral signatures that are discontinuous for mass and NMR spectra and continuous for UV and IR spectra and thus need to be transformed (e.g. sampling, Fourier transform), and (iv) quantum variables (isopotential map, charge or π electron densities, free valence index, etc.). Algorithms similar to certain pattern recognition techniques are then used to identify discriminant structural groups.

Since the application of these methods inevitably requires the assistance of a theoretical chemist, an approach that enables the life-scientist if only to classify chemical structures unaided and observe structural affiliations would be most welcome. Such techniques based on cluster analysis[47] that do not require a prior rigorous molecular description are indeed available. For the purposes of the analysis of the data in Table II, we shall describe one of the simpler cluster techniques, the minimum spanning tree (MST),[39,47-49] which is used here to describe the organisation of the 37 molecules when projected into a multidimensional space defined by the seven biological properties.

The objective is to generate a 2D planar graph from the normalized 7D data table that best describes the nearest-neighbor relationships among the test compounds. To do this, the raw data matrix is first converted into a symmetric semi-matrix of the χ^2 distances separating each pair of compounds (see the Experimental Section). From this starting point, in which each of the n molecules can be considered a group, a series of mergers are operated by single-link clustering that terminates with a single group constituted of all n molecules arranged in a network. This network spans all items by a set of straight lines joining pairs of points whose lengths are equal to the appropriate interpoint distances. The Prim algorithm[39] we have used seeks the closest neighbor V_1 (shortest edge in graph theory) to an item (vertex V). This operation is reiterated, the kth step consisting in adding to the existing V_{k-1} edges the shortest edge V_k which can be linked to a vertex within V_{k-1} without forming a closed loop. After $n-1$ iterations, a minimum spanning tree has been created. In this final tree, the overall activity profile varies least between a molecule and its nearest neighbor. The overall distance separating two molecules, as measured along the pathways generated, reveals how close is the relationship between them with regard to all the biological parameters measured. A novel activity profile leads to a branching out from the network.

The criterion that the sum of the segments linking the molecules be as small as possible is far from trivial if one considers that there are nearly 500 million ways in which 12 items can be arranged in linear order. The number of ways 37 molecules can be arranged into a branched network is cosmic! The MST, which is the single network that best describes the data matrix, is thus not just a logical way of disposing the items but a true description of the inherent structure of the system under study (e.g. refs 50 and 51).

The clear visual impact of the MST form of data representation and interpretation is not the least of its advantages (Figure 4): (a) The position of a molecule, i.e. part of a trunk or a branch, a main branch or a twig, at a bifurcation or within a long stem, indicates whether the molecule is part of a cluster of similar molecules, an intermediate within a stepwise progression, or a new lead compound. Its common denominator with other molecules can be deduced. (b) The MST in Figure 4 classifies the chemical structures on the basis of their selectivity with regard to the tests (see Figure 5 below) but not their absolute activity levels. The pathways along the branches (see Figure 6 below) illustrate how the properties of the molecules evolve with structure. If the properties measured are interactions with specific proteins, contiguity between molecules can reflect analogies in active sites of ligands.[52] (c) The full biological profile of a new molecule can be introduced into the system to determine the location of this molecule with respect to the others.

Minimum Spanning Tree of the Test Molecules. The MST of the test molecules (Figure 4) was constructed on the basis of specificity profiles as shown in Figure 5 for

(43) Nishizuka, Y. The role of protein kinase C in cell surface signal transduction and tumor promotion. *Nature* **1984**, *308*, 693.
(44) Nishizuka, Y. Studies and prospectives of the protein kinase C family for cellular regulation. *Cancer* **1989**, *63*, 1892.
(45) Broto, P.; Moreau, G.; Vandycke, C. Molecular structures: perception, autocorrelation descriptor and sar studies. Perception of molecules: topological structure and 3-dimensional structure. *Eur. J. Med. Chem.* **1984**, *19*, 61.
(46) Dubois, J. E.; Laurent, D.; Bost, P.; Chambaud, S.; Mercier, C. Système DARC. Méthode DARC/PELCO. Stratégies de recherche de corrélations appliquées à une population d'adamantanamines antigrippales (DARC system. DARC/PELCO method. Strategy for seeking correlations as applied to a population of anti'flu adamantanamines). *Eur. J. Med. Chem.-Chim. Ther.* **1976**, *11*, 225.
(47) Chatfield, C.; Collins, A. J. Multidimensional scaling and cluster analysis. In *Introduction to Multivariate analysis*; Chapman and Hall: London, 1989; p 189.
(48) Gower, J. C.; Ross, G. J. S. Minimum spanning trees and single linkage cluster analysis. *Appl. Statist.* **1969**, *18*, 54.
(49) Barthélémy, J. P.; Guénoche, A. Les arbres et les représentations des proximités (Trees and proximity representations). Masson, Paris, 1988, p 1.
(50) Devillers, J.; Doré, J. C. Heuristic potency of the minimum spanning tree (MST) method in toxicology. *Ecotox. Environ. Safety* **1989**, *17*, 227.
(51) Doré, J. C.; Lacroix, J.; Lacroix, R.; Viel, C. De la manipulation informatique des formules developpées pour l'étude des relations structure-activité. Application aux médicaments antiparasitaires (The manipulation of information of developed formulas for the study of structure-activity relationships. Application to antiparasitic agents). *J. Pharm. Belg.* **1990**, *45*, 375.
(52) Ojasoo, T.; Mornon, J. P.; Raynaud, J. P. Steroid hormone receptors. In *Comprehensive Medicinal Chemistry*; Emmett, J. C., Ed.; Pergamon Press: Oxford, 1990; Vol. 3, p 1175.

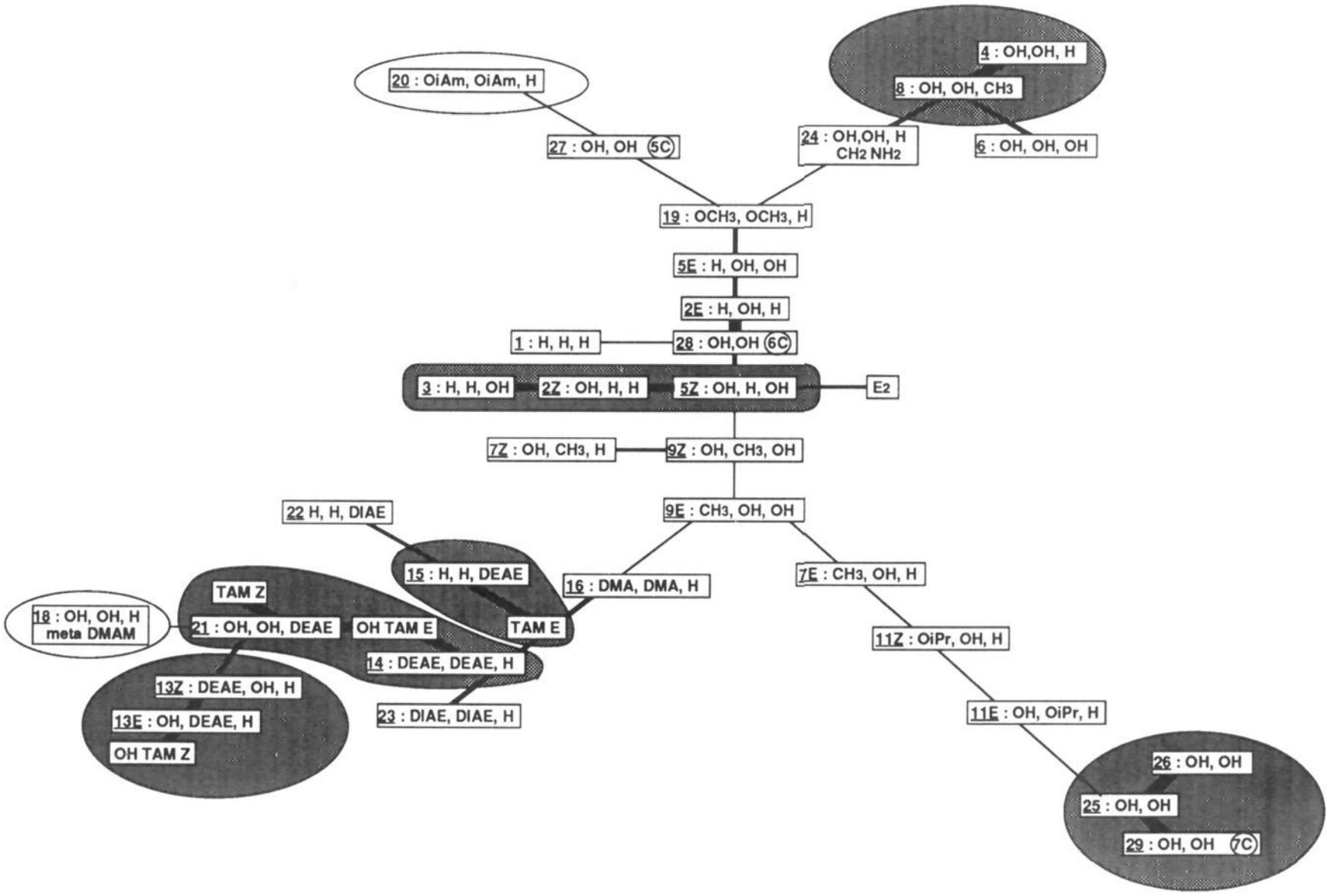

Figure 4. Minimum spanning tree of the TPE structures constructed on the basis of specificity of response. Typical specificity profiles are shown in Figure 5. The relative proximity of two TPEs is indicated by the nature of the line linking them: broad line, very close; medium line, close; fine line, distant. Clusters of molecules with highly similar activity profiles are encircled and hatched. Isolated molecules are just encircled.

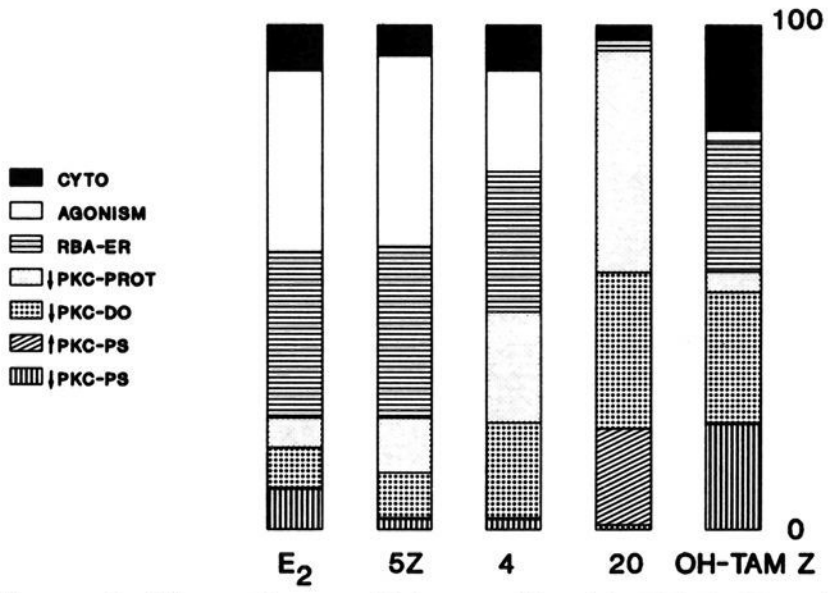

Figure 5. Illustrative specificity profiles (E_2, 5*Z*, **4**, **20**, and OH-TAM *Z*) forming the basis of the minimum spanning tree in Figure 4.

the reference compounds E_2 and 5*Z* and for the tip-of-the branch compounds **4**, **20**, and OH-TAM *Z*. The MST has a main trunk and four branches of unequal length. At the center of the tree, in an offshoot off the main trunk, one can locate the reference molecule estradiol (E_2). Its only neighbor, and counterpart in the TPE series, is the α,β-dihydroxylated TPE 5*Z* that has the closest selectivity profile to E_2 (Figure 5) and forms part of the main trunk. TPE 5*Z* is most closely related to TPEs 2*Z* and **3** (see cluster in Figure 4), somewhat less closely related to the duo DPE **28** (with a 6-carbon ring) and TPE 2*E*, and more distantly related to TPEs 9*Z* and 7*Z*. To our knowledge, the crystal structure of 5*Z* is not available but that of 7*Z*

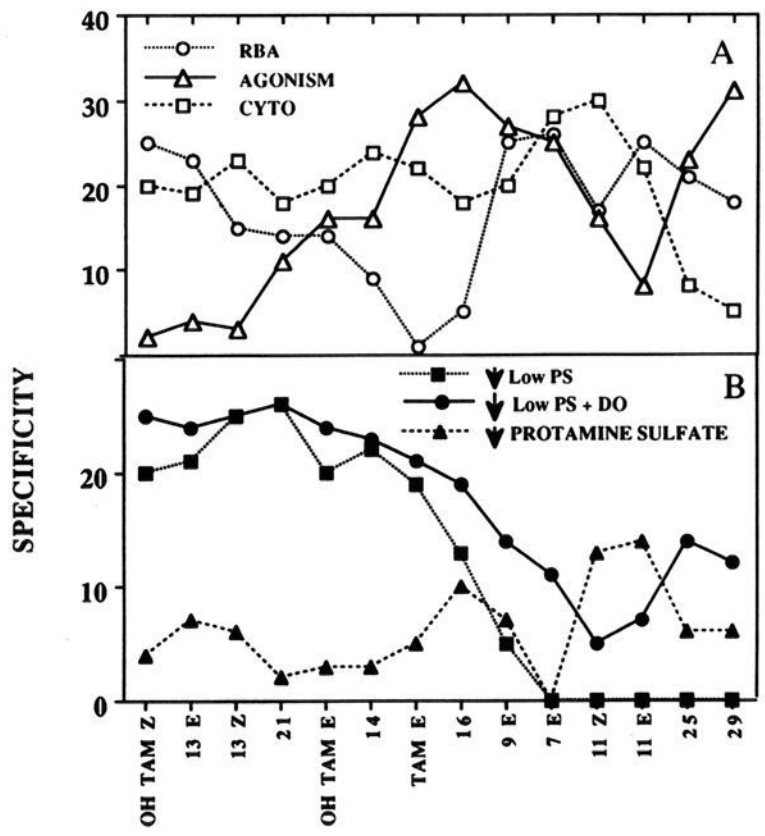

Figure 6. Specificity profiles of the molecules along the pathway from OH-TAM Z to DPE **29** in the minimum spanning tree of Figure 4. (A) ER binding and cell proliferation, (B) PKC activity.

has been superimposed with E_2.[9,53] Superposition of either the α or the β ring of TPE 7*Z* with the A ring of E_2 are

(53) Pons, M.; Bignon, E.; Crastes de Paulet, A., Gilbert, J.; Ojasoo, T.; Raynaud, J. P. Hydroxylated triphenylacrylonitriles adopt a unique orientation with the binding site of the estrogen receptor. *J. Steroid Biochem.* **1990**, *36*, 391.

equally satisfactory although biochemical data would suggest that the main anchorage point of TPEs in the hormone binding site of ER is preferentially the α-phenolic ring.[53] The proximity between E_2 and **5*Z*** suggests that the flexible TPE skeleton might be a handy prop to test the effects of diverse chemical substituents besides hydroxy groups on a variety of molecular targets as it has a greater number of degrees of freedom than the steroid skeleton. To our knowledge, there is no published evidence of PKC inhibition by steroid derivatives.

Of particular note is the dispersion of the DPEs within the tree. DPE **28** (deacetylated cyclofenil) constitutes the essential link leading from the E_2-mime, **5*Z***, toward test compounds that are selective PKC agents such as DPE **27** (top left-hand branch) or that are noncytotoxic agonists that interact with both ER and PKC (top right-hand branch). On the other hand DPEs **25**, **26**, and **29** are reached by a bifurcation at **9*E*** resulting from a more marked contribution of stimulation of PKC-PS activity, RBA and agonist activity and some cytotoxicity (**7*E*** and **11*Z***) (see Figure 6 below). Some of these differences in specificity profiles can only be due to differences in ring structure: **27** has a rigid envelope-structure 5-membered carbon ring, **28**, a flexible "flip-flap" 6-carbon ring, and **29**, a constrained 7-carbon ring.

Several clusters of two to four TPEs with comparable selectivity profiles can be identified: TPEs **4** and **8**; TAM *E* and TPE **15**; TPEs **14** and **21**, OH-TAM *E*, and TAM *Z*; TPEs **13*Z*/*E*** and OH-TAM *Z*; DPEs **25**, **26**, and **29**. These clusters highlight the number of "me-too's" with analogous specificity profiles that have been designed within this small population of molecules. On the other hand, two TPEs are situated at the end of remote tips, i.e., TPEs **18** (the only metasubstituted TPE in the series) and **20** (an α,α'-diisoaminoethyl derivative). Their activity profiles (lack of ER binding in both cases, but differential actions on agonism and PKC stimulation) are uncommon within this population.

The pathways leading from TPE **9*E*** (center) to the reference "anti-estrogen" OH-TAM *Z* (left) and to DPE **29** (right) are depicted in Figure 6. Toward the left, one notes an increasing contribution with structural change (bulky N-containing substituents) of inhibition of Ca^{2+}- and phospholipid-dependent PKC phosphorylation of H_1 histone especially in the presence of DO, appreciable but invariant cytotoxicity, a parabolic change in RBA for ER, and a steady decrease in agonist activity. Toward the right, the specificity profiles are very different with an interesting transition occurring between TPEs **7*E*** and **25**. Whereas cytotoxicity peaks, agonism passes through a trough.

A more evocative representation is given by the geological-type strata of Figure 7. The difference between the profiles in Figure 7 and those in Figure 6 lies not only in the representation form (cumulated values) but in the fact that account is taken of the overall activity of each molecule. Thus Figure 7 reflects not only specificity of effect as in Figure 6 but also amplitude of effect. It is to be noted, however, that as described in the legend in Table II the effects observed occur at different concentrations.

Overall, one observes trends toward absence of cytotoxicity toward the tree-top especially in the left-hand branch compared to cytotoxicity at the bottom, stimulation of PKC in the bottom right-hand branch only, and agonism (cell-proliferation) virtually throughout with the notable exception of **20** and, to a lesser degree, of OH-TAM *Z*. This agonism is even manifest in compounds lacking any significant contribution from ER binding (e.g. **18**, **22**, **15**, TAM *E*). Because the affinity of these compounds is very

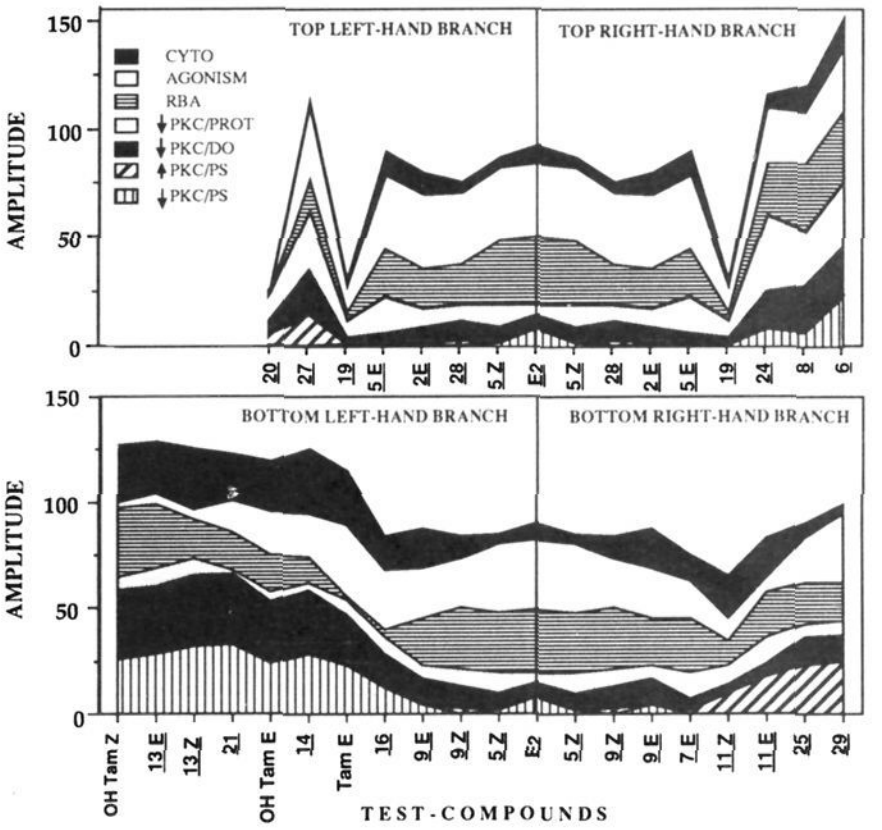

Figure 7. Relative activity profiles of the molecules along the four branches of the minimum spanning tree of Figure 4 starting from E_2 in the middle. In the top panel the first five molecules (**5*Z*** to **19**) are common to both left and right branches; in the bottom panel only three molecules (**5*Z*** to **9*E***) are common to both lower branches.

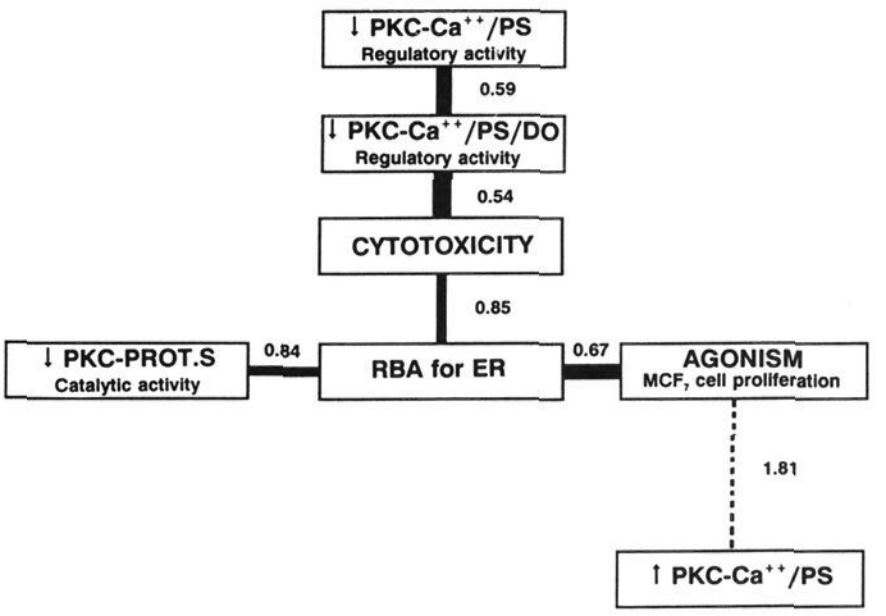

Figure 8. Minimum spanning tree describing the relationships among the biological variables. The tree was constructed on the basis of the data in Table II. The distances between the variables indicate the closeness of a relationship.

low, extremely high concentrations are needed for cell proliferation, but the hypothesis that ER may not be the sole molecular target accounting for the cell proliferation they induce should not be totally rejected. When agonism is high, cytotoxicity is low. Furthermore, a certain parallelism between cytotoxicity and PKC inhibition in the presence of diolein is apparent. On the other hand, there is no consistent association between PKC activity and growth as exemplified by the absence of agonism of **20**.

Minimum Spanning Tree of the Biological Variables. A MST was also calculated to further our understanding of the relationships among the biological variables for this population of molecules. These relationships have already been described in detail in a previous paper based on another type of multivariate analysis (correspondence factorial analysis (CFA)).[38] The MST largely confirms the results of the CFA. Briefly, TPE competition for ER binding is related to the ability to promote MCF_7 cell

growth and, to much lesser extents, to the ability to inhibit PKC phosphorylation of protamine sulfate (i.e. the presumably catalytic activity of PKC) and to kill MCF_7 cells at high concentrations. Although some relationship can be established between ER binding and TPE cytotoxicity, this latter parameter is more closely related to TPE inhibition of PKC phosphorylation of H_1 histone that occurs in the presence of Ca^{2+} and phosphatidylserine (PS) (i.e. the presumably regulatory activity of PKC), when this phosphorylation is measured in the presence of diacylglycerol (diolein = DO). In the absence of DO, the natural activator of PKC, the relationship is more distant ((0.54 + 0.59) vs 0.54). Stimulation of PKC is highly remote from the other variables and, naturally, situated at the opposite end of the trunk with respect to PKC inhibition.

As noted previously,[38] the two most unexpected relationships revealed by this multivariate analysis are the proximity of TPE cytotoxicity and PKC inhibition in the presence of DO and the remote position, in the vicinity of RBA, of inhibition of PKC phosphorylation of protamine sulfate.

Experimental Section

Melting points were determined on a Kofler apparatus and are uncorrected. Elemental analyses of all new compounds were performed in the Microanalytical Laboratory of the CNRS (Vernaison, France). Results were within ±0.3% of the theoretical values for those elements shown. ^1H NMR spectra were recorded (δ 0) at 90 or 300 MHz on a Bruker spectrometer with Me_4Si as internal standard. IR spectra were determined with a Beckman ACCULAB IV. Thin-layer chromatography was performed on silica gel 60 F_{254} precoated aluminum sheets. A Waters apparatus was used for analytical HPLC.

Synthetic Procedures. 2-Phenyl-3-(4-hydroxyphenyl)-3-[4-(isoamyloxy)phenyl]acrylonitrile (Mixture of *E* and *Z* Isomers) and 2-Phenyl-3,3-bis[4-(isoamyloxy)phenyl]acrylonitrile (20). 2-Phenyl-3,3-bis(4-hydroxyphenyl)acrylonitrile (5 g, 16 mmol) was added under a stream of nitrogen to a stirred solution of sodium ethoxide (368 mg Na, 0.016 atom) in absolute ethanol (80 mL). 1-Bromo-3-methylbutane (3.02 g, 20 mmol) was then added slowly. After heating to reflux for 7 h, the reaction mixture was cooled and treated with H_2O (100 mL), concentrated in vacuo, and extracted with CH_2Cl_2. The combined organic layers were washed and dried (Na_2SO_4). After removal of the solvent, the resulting crude product (5.6 g) was chromatographed on a silica gel column (eluent: CH_2Cl_2/EtOAc, 95:5). Four compounds were successively identified. (1) The bis-substituted compound **20** (0.37 g): TLC (same eluent) R_f 0.82; mp 111 °C (EtOH). Anal. Calcd for $C_{31}H_{35}NO_2$: C, 82.11; H, 7.72; N, 3.09. Found: C, 82.08; H, 7.28; N, 2.77. (2–3) A mixture of *E* and *Z* isomers (2.30 g): TLC ($CHCl_3$/CH_3OH/TEA, 95:3:2) R_fs 0.60 and 0.48; mp 132–134 °C (cyclohexane); IR ($CHCl_3$) 3570–3200 (OH), 2200 (CN) cm^{-1}; ^1H NMR ($CDCl_3$) (90 MHz) δ 0.86 (d, CH_3, *Z* isomer, 45%), 0.93 (d, CH_3, *E* isomer, 55%), 1.6–2.08 (m, 3 H, $CHCH_2$), 3.87 (t, OCH_2, *E* isomer), 3.97 (t, OCH_2, *Z* isomer), 4.98 (large s, OH), 5.46 (large s, OH), 6.48–7.42 (m, 13 H, arom). Anal. Calcd: C, 81.46; H, 6.52; N, 3.65. Found: C, 81.17; H, 6.68; N, 3.56. (4) The fourth compound was the starting bis-hydroxy derivative (1.30 g).

2-[4-[2-(Diethylamino)ethoxy]phenyl]-3,3-bis(4-hydroxyphenyl)acrylonitrile (21). The synthesis was in two steps, the first step being the preparation of 4,4′-bis(tetrahydropyran-2-yloxy)benzophenone. Concentrated H_2SO_4 (two drops) was added to a suspension of 4,4′-dihydroxybenzophenone (10.7 g, 50 mmol) in 3,4-dihydro-2*H*-pyran (50 mL). After stirring for 15 h at room temperature, the reaction mixture was extracted twice with benzene. The combined organic layers were treated with Na_2CO_3 solution (10%) until neutralization, washed with water, and dried (Na_2SO_4). The solvent was removed, and the residual oil was crystallized (sulfuric ether/pentane, 1:3): yield 10 g (52%); mp 103–104 °C. Anal. Calcd for $C_{23}H_{26}O_5$: C, 72.25; H, 6.80. Found: C, 72.27; H, 7.01.

A solution of [4-[2-(diethylamino)ethoxy]phenyl]acetonitrile[54] (3.5 g, 15 mmol) in anhydrous ether (50 mL) was added dropwise under nitrogen to a warm suspension of sodium amidure (1.2 g, 30 mmol) in anhydrous ether (50 mL). After heating for 2 h, the reaction mixture was cooled to room temperature at which point a solution of the above-prepared 4,4′-bis(tetrahydropyran-2-yloxy)benzophenone (4 g, 10 mmol) in anhydrous ether (50 mL) was added. The mixture was stirred, heated under reflux for 8 h, and then cooled before addition of water. Ether and water were eliminated and CH_3OH was added (70 mL). After acidification with HCl (30%) to pH 1 and after 2 h standing, the CH_3OH was eliminated in vacuo with ether, and a solution of HCl (10%) was added. Extraction with ether (50 mL × 2) gave an aqueous layer containing the basic compound which was alkalinized with 10% NaOH to pH 11 and treated with ether (50 mL × 2). A first extraction by $CHCl_3$ (100 mL) was followed by slow addition of diluted HCl to pH 7–8 and reextraction (twice) with $CHCl_3$ (100 mL × 2). The combined organic layers were washed with water and dried (Na_2SO_4). After removal of solvent, the residual oil was crystallized from a mixture of sulfuric and petroleum ethers to give 2.5 g of a mixture of two compounds [TLC (CH_2Cl_2/CH_3OH/TEA; 20:5:0.25), R_fs 0.43 and 0.25]. **20** was obtained by chromatography over a silica gel column (60, 200–400 mesh) eluted by CH_3Cl/TEA (99:1) and increasing proportions of CH_3OH (R_f 0.43): mp 135–7 °C; IR (KBr) 3500–3000 (OH), 2200 (CN) cm^{-1}; ^1H NMR δ 1.05 (t, 6 H, CH_2CH_3), 2.77 (q, 4 H, CH_2CH_3), 3.01 (t, 2 H, CH_3CH_2N), 4.1 (t, 2 H, OCH_2), 6.59–7.24 (m, 12 H, arom), 9.85 (s, OH), 10 (s, OH).

2-[4-[2-(Diisopropylamino)ethoxy]phenyl]-3,3-diphenylacrylonitrile (22). 2-(4-Hydroxy-phenyl)-3,3-diphenylacrylonitrile was prepared by demethylation of the corresponding methyl ether. A mixture of this phenol (4 g, 13.5 mmol), 2-(diisopropylamino)ethyl chloride hydrochloride (7.4 g, 37 mmol) and anhydrous potassium carbonate (9.30 g, 67.5 mmol) in anhydrous acetone (200 mL) was stirred and heated for 20 h under nitrogen. A mineral solid was separated by filtration. The solution was concentrated, and the residue was diluted with water and extracted with ether. The organic phase was washed, treated with a 5% NaOH solution, washed with water, and dried (Na_2SO_4). After concentration, the residue was chromatographed on silica gel (elution with $CHCl_3$/CH_3OH, 90:10). The separated oil was distilled (250–5 °C (0.01 mm Hg)): ^1H NMR ($CDCl_3$) (90 MHz) δ 1.04 (d, 12 H, CH_3), 2.66–3.22 (m, 4 H, $CH_2N(CH)_2$), 3.86 (t, OCH_2), 6.57–7.55 (m, 14 H, arom). Anal. Calcd for $C_{29}H_{32}N_2O$: C, 82.07; H, 7.57; N, 6.60. Found: C, 82.49; H, 7.71; N, 6.59.

2-Phenyl-3,3-bis[4-[2-(diisopropylamino)ethoxy]phenyl]acrylonitrile (23). 2-Phenyl-3,3-bis(4-hydroxyphenyl)acrylonitrile was prepared by demethylation of the corresponding dimethyl ether. This diphenol (5 g, 16 mmol) was added under nitrogen to a stirred suspension of (diisopropylamino)ethyl chloride hydrochloride (19.6 g, 98 mmol) and K_2CO_3 (22.17 g, 160 mmol) in anhydrous acetone (250 mL). Stirring and reflux were maintained for 22 h. After cooling, the reaction mixture was filtered (NaCl) and the solution was concentrated in vacuo. The residue was extracted with ether (200 mL × 2). The combined organic layers were acidified with diluted HCl. The aqueous solution was alkalinized with a 5% NaOH solution and extracted with ether (200 mL × 2). The organic solution was washed with water, dried (Na_2SO_4), and concentrated. The residue was chromatographed twice on a silica gel column (60, 200–400 mesh). Elution with $CHCl_3$ containing increasing proportions of CH_3OH gave **23** as an oil (4.35 g, 48%): ^1H NMR ($CDCl_3$) (90 MHz) δ 0.95 (d, 12 H, CH_3), 1.02 (d, 12 H, CH_3), 2.66–3.33 (m, 8 H, 2 [(CH)(CH)NCH$_2$]), 3.82 (t, 4 H, OCH_2), 6.46–7.40 (m, 13 H, arom). Anal. Calcd for $C_{37}H_{49}N_3O_2$: C, 78.30; H, 8.64; N, 7.40. Found: C, 78.17; H, 8.48; N, 7.18.

Biology: Other Chemicals and Materials. TAM and 4-OH-TAM isomers were kind gifts from Dr. A. H. Todd (ICI, Macclesfield, England). [6,7-^{3}H]E_2 (1.85 TBq/mmol) was from the Commissariat à l'Energie Atomique (France). All materials for the binding and activity assays were obtained from the sources

(54) Hughes, G. M. K.; Moore, P. F.; Stebbins, R. B. Some hypocholesteremic 2,3,1-diphenylacrylonitriles. *J. Med. Chem.* **1964**, *7*, 511.

given in the relevant publications describing the assays.[36,37] Solutions of all test compounds in 95% alcohol were stored at 4 °C in the dark for no longer than 2 weeks and checked before use by thin-layer chromatography (CH_2Cl_2/hexane, 90:10, v/v) or by high-performance liquid chromatography (HPLC).

Biological Screening Methods. The relative binding affinities (RBAs) of the test compounds for calf uterus cytosol estrogen receptor (ER) were measured after incubation for either 2 h at 0 °C or 5 h at 25 °C by a competition method using [6,7-^{3}H]-17β-estradiol (RBA of estradiol = 100%) as previously described.[36]

Growth stimulation and cytotoxicity in MCF_7 (ER-positive) human breast cancer cells were studied in 24-well tissue-culture cluster plates as previously described[36] using culture medium without phenol red containing 5% dextran-coated charcoal.

Purified Type III (α) PKC was separated from rat brain soluble fraction[55] and assayed according to published procedures[37] under three different activation conditions, i.e., using calf thymus H_1 histone as substrate in the presence of 0.1 mM Ca^{2+}, 5 mM magnesium acetate, 10 μM [^{32}P]ATP, or 2 μg/mL of phosphatidylserine (PS) with or without 0.2 μg/mL of diolein (DO), or using protamine sulfate as substrate in the presence of 0.5 mM EGTA instead of Ca^{2+}, PS, and DO.

Multivariate Statistical Analysis. The results in Table II on the responses of 37 compounds (rows) in seven tests (columns) were analyzed by the minimum spanning tree (MST) method.[39] First, the result for each compound was expressed as a percentage of the maximum value recorded in each test (multidimensional scaling from 1 to 100) in order to spread out the statistical weight attributed to each test evenly. Second, this transformed result was then expressed as a further percentage of the sum total of the transformed values recorded for the compound in the seven tests. In other words, for each test compound, the final contributions of each biological variable to the overall response profile totalled 100%. Third, the transformed data matrix was converted into a matrix of χ^2 distances between pairs of compounds, i.e. the distances separating two molecules when there are projected into the 7-dimensional space defined by the orthogonal axes characterising the tests (see the supplementary material). The conversion giving a symmetrical 37 × 37 semimatrix is performed using the formula

$$\delta^2(i,i') = \sum_{j=1}^{7}\left[\frac{1}{p{\cdot}j}\left(\frac{pij}{pi{\cdot}} - \frac{pi'j}{pi'{\cdot}}\right)\right]^2$$

The square of the distances between two molecules i and i' is equal to the summed squares for the seven tests of the difference between the response (pij) of molecule i for test j divided by the overall response profile ($pi{\cdot}$ or $pi'{\cdot}$) of molecule i or i' for all tests; this difference is multiplied by the reciprocal of the profile of each test $p{\cdot}j$. The χ^2 distances were calculated on a PC-AT compatible microcomputer (640 Ko of central memory) by a program written in BASIC Microsoft. This mathematical ploy converts the individual hierarchies of response of the 37 compounds on each of the seven tests into a single descriptive organisation. Third, in order to organize the molecules according to their similarities/dissimilarities in response profiles, the shortest distance linking them into a network (no loops nor backtracking allowed) was calculated by the Prim algorithm for the construction of a minimum spanning tree.[39] The tree is linear only if the seven variables are perfectly autocorrelated (e.g seven ways of measuring the same phenomenon). This methodology can be reasonably applied to data matrices for several hundred molecules and up to a maximum of 100 biological variables. With an AT386 computer fitted with an arithmetical processor, the calculation time is a few minutes for the smaller matrices and up to several hours for a 500 × 100 matrix. The program is available upon request from J. C. Doré.

Acknowledgment. We thank Professor Y. Nishizuka (Department of Biochemistry, Kobe University School of Medicine, Japan) for his cooperation in this study. The PKC data were obtained in his laboratories.

Registry No. 1, 6304-33-2; 2*Z*, 19460-09-4; 2*E*, 84836-12-4; 3, 16143-90-1; 4, 66422-14-8; 5*Z*, 16144-07-3; 5*E*, 16144-06-2; 6, 76621-40-4; 7*Z*, 84836-13-5; 7*E*, 84836-14-6; 8, 90468-83-0; 9*Z*, 90468-84-1; 9*E*, 90468-85-2; 10*Z*, 118976-11-7; 10*E*, 118976-10-6; 11*Z*, 118976-13-9; 11*E*, 118976-12-8; 12, 118976-14-0; 13*Z*, 104575-13-5; 13*E*, 104575-22-6; 14, 118976-15-1; 15, 118976-16-2; 16, 118976-17-3; 18, 121425-55-6; 19, 66422-13-7; 20, 137743-23-8; 21, 137743-24-9; 22, 137743-25-0; 23, 137743-26-1; 24, 66422-11-5; 25, 66422-07-9; 26, 66422-17-1; 27, 66422-10-4; 28, 5189-40-2; 29, 14303-48-1; TAM *Z*, 10540-29-1; TAM *E*, 13002-65-8; 4-OH-TAM *Z*, 65213-48-1; 4-OH-TAM *E*, 68047-06-3; E_2, 50-28-2; PK, 9026-43-1; 2-phenyl-3,3-bis(4-hydroxyphenyl)acrylonitrile disodium salt, 137743-27-2; 1-bromo-3-methylbutane [4-[2-(diethylamino)ethoxy]phenyl]acetonitrile, 92373-69-8; 4,4′-bis(tetrahydropyran-2-yloxy)benzophenone, 133088-86-5; (diisopropylamino)ethyl chloride, 96-79-7; 2-(4-hydroxyphenyl)-3,3-diphenylacrylonitrile, 137743-28-3; 4,4′-dihydroxybenzophenone, 611-99-4; 3,4-dihydro-2*H*-pyran, 110-87-2.

Supplementary Material Available: χ^2 distance matrix (1 page). Ordering information is given on any current masthead page.

(55) Sekiguchi, K.; Tsukuda, M.; Ase, K.; Kikkawa, U.; Nishizuka, Y. Mode of activation and kinetic properties of three distinct forms of protein kinase C from rat brain. *J. Biochem.* 1988, *103*, 759.